Printed pH Sensors for Textile-Based Wearables: A Conceptual and Experimental Study on Materials, Deposition Technology, and Sensing Principles

Peer-reviewed author version

JOSE, Manoj; MYLAVARAPU, Satish Kumar; Bikkarolla, Santosh Kumar; MACHIELS, Jarne; Sankaran, K. J.; McLaughlin, James; HARDY, An; THOELEN, Ronald & DEFERME, Wim (2022) Printed pH Sensors for Textile-Based Wearables: A Conceptual and Experimental Study on Materials, Deposition Technology, and Sensing Principles. In: ADVANCED ENGINEERING MATERIALS, 24(5), (Art N° 2101087).

DOI: 10.1002/adem.202101087
Handle: http://hdl.handle.net/1942/36333

Printed pH Sensors for Textile-Based Wearables: A Conceptual and Experimental Study on Materials, Deposition Technology and Sensing Principles

*Manoj Jose, Satish Kumar Mylavarapu, Santosh Kumar Bikkarolla, Jarne Machiels, Sankaran K J, James McLaughlin, An Hardy, Ronald Thoelen, Wim Deferme **

*Correspondance: wim.deferme@uhasselt.be

M. Jose, J. Machiels, R. Ronald, W. Deferme

Hasselt University, Institute for Materials Research (IMO-IMOMEC) 1, 3590 Diepenbeek, Belgium

IMEC, Division IMOMEC, Wetenschapspark 1, B-3590 Diepenbeek, Belgium

S.K. Mylavarapu, A. Hardy

Hasselt University, Institute for Materials Research (IMO-IMOMEC) 1, 3590 Diepenbeek, Belgium

IMEC, Division IMOMEC, Wetenschapspark 1, B-3590 Diepenbeek, Belgium

Energyville, Thor Park 8320, Genk, B-3600 Belgium

S. K. Bikkarolla, J. McLaughlin

School of Engineering, Engineering Research Institute, University of Ulster, Newtownabbey BT37 0QB, UK

Sankaran K. J.

CSIR-Institute of Minerals and Materials Technology, Bhubaneswar 751013, India

Abstract

This article investigates organic and polymeric materials, printing technology and sensing principles towards a reliable printed wearable pH sensor realised on textile substrates. This work systematically makes a literature study and experimental work of three different organic and polymeric material based pH sensors and their corresponding measurement methods. Initially, the three different sensors, a conductometric PEDOT:PSS sensor, a voltammetric carbon-alizarin sensor and a potentiometric PANI sensor were selected based on certain established criteria and were reproduced on foils for a feasibility study. Mass but simple production, and feasibility for fabrication on textile substrates were also being

This article has been accepted for publication and undergone full peer review but has not been through the copyediting, typesetting, pagination and proofreading process, which may lead to differences between this version and the Version of Record. Please cite this article as doi: 10.1002/adem.202101087

the objectives of this work, and led to the deployment of printing and coating techniques for the sensor fabrication. These three sensors were printed on flexible foils and tested and verified for sensor performances. The performance measures like sensitivity, linearity and repeatability of the sensors and their mechanical properties were investigated with prime importance. Based on the experimental results together with a literature study, a conclusive comparison between the sensing principles with respect to device fabrication, functionality and wearability were performed. As per this analysis, one principle was chosen and further developed towards a textile-based printed sensor. A potentiometric graphene/PANI sensor was printed on a textile substrate and tested for a buffer solution of pH ranging from 4 to 10. The potentiometric sensor based on PANI shows a 45mV/pH sensitivity with linear sensor responses and repeatable characteristics. It proves as a potential pH sensor on textiles for wearable health applications.

Keywords: Printed electronics, pH sensor, Textile, Wearable electronics, Organic and polymers

1. Introduction

Human biofluids contain numerous known physical and chemical biomarkers that play a vital role in diagnosing the humans health status. In healthy conditions, these biofluids maintain a strict pH balance with an efficient regulation, and slight changes in pH can be used as an early detector of malfunction or disease. Sweat is such a biofluid and normal sweat has a pH in the range of pH 4.5 to 6.8[1]. It is possible to track dehydration[2-3] or risk of diabetes[4] and detect cystic fiberosis[5] with the pH readings of perspiration/sputum/urine. Similarly, wound healing is a complex dynamic and multifaceted process consisting of hemostasis, inflammation, proliferation, and remodeling stages[6]. During these different stages, the wound fluid pH could vary between 4.5 to 8.5,[7-8] depending on the type of wound and its complexities in healing. A recent report indicates that the wound management expenditure has grown up to 4% of the health budget contribution in Europe[9]. However, with the help of accurate determination of the wound's pH, very essential physiological information can serve as a source to simplify the entire wound diagnosis and treatment practice[10-12].

pH is a measure of acidity or basicity, and in 1909 Sørensen defined the pH scale as the H^+ ion molar concentration on a negative logarithm scale[13]. In the same year, scientiests developed a pH sensitive glass electrode[14]. Arnold Beckman designed the very first commercial pH measurement system in 1936, which brought about the production of commercial pH meters[15]. It consisted of glass electrodes where the potential difference between the working and reference electrodes indicate the analyte's pH. Those sensor systems are highly sensitive to H^+ ions and stable, however, they are fragile, bulky and do

not have a suitable form factor to be incorporated for human body in situ measurements. pH sensors for body measurements are preferred to be flexible, lightweight, and low cost with decent working range of operation. Along with this, selectivity to H^+ ions and biocompatibility are the foremost sensor desirable attributes. Paper based pH indicators are known for a long time as a rapid, simple and easy technique to make pH sensing. The paper, treated with flavin (organic compound group), turns its colour from red over yellow to green due to redox changes when it is dipped in low pH over neutral to high pH solutions respectively. Although paper's mechanical properties comply with the skin, this method is mostly limited due to inaccuracies and reproducibility matters.

Optical principle based sensors are attractive due to features like feasibility to miniaturize, no electrical interference, high sensitivity and remote sensing capabilities. Yet, the sensors expensive setup, complex labeling process, cross sensitivity to ionic strength and very limited range of measurements are down sides[15-17]. Electrochemical techniques such as voltammetric, potentiometric and conductometric principles have shown great potential in terms of good sensitivity, extensive range and viability to be a flexible sensor[18-19]. Iridium oxide (IrO_2) is the most studied, electrochemical pH sensing material. IrO_2 electrodeposited flexible potentiometric sensors have shown a pH sensitivity of 72.5 mV/pH in the range of pH from 3-11 and the same material dip-coated sensor shows a sensitivity of 51 mV/pH over the pH range from 2-12[20]. Apart from IrO_2, other electrochemical MO_x sensors made up of TiO_2[21], RuO_x[22], WO_3[23], and ZnO[24] are also distinguished as pH sensitive and promising material choice. The MOx sensors are reported to be deposited using different techniques such as electron beam evaporation, sputtering, electrodeposition and dip coating[19].

Conventional microfabrication routes are complex, time consuming, expensive and not the best fit for the fabrication of textile sensor applications. Although spin coating has been chosen often for device fabrication in lab scale, it is not ideal for textiles, misfit for volume production and also causes huge material wastage[25]. Contemporarily, printed electronics grabbed more attention as an industry viable production technology, especially towards flexible electronics and innovative textile applications. Some of the major works in connection with intelligent textile-based wearable sensors for different sensing attributes reported in the literature include the wearable strain sensor developed on graphene textile without polymer encapsulation[26]; worm-shaped graphene monolayer enabled ultrahigh tensile strain and stable conductance[27]; integrated smart textile bands for self-pumping sweat sampling and analysis[28]; integrated smart clothing by employing multiscale disordered porous elastic fibers as sensing units capable of autonomous self-sensing of strain and temperature and self-cooling[29]; and bio-inspired textile sensor with conical micropores for human body moisture and thermal management[30]. As a compatible textile production processing method in ambient air, it emphasizes printing and coating as the future of manufacturing technology[31].

Electrochemical MOx sensors are described for printing and coating based material deposition to produce pH sensors . However, the MOx sensors are yet to prove the repeated flexing and bending capabilities and also the high curing temperature is a challenge for textile sensors[19, 32-33]. Moreover, the metal oxide sensors have shortcomings in sensor characteristics like hysteresis, drift and cross-sensitivity that restrict them to be used in health monitoring applications[34]. Studies of Alam et al. highlight major pH sensor works based on electrochemical organic compounds and conductive polymers to be a better

alternative for wearable biomedical applications[35]. Many of these materials are solution-processable, intrinsically flexible, cheap and suitable for wearable textiles [12, 36-39]. Among this, PANI is an intrinsically pH-sensitive, conductive polymer with good environmental stability and biocompatibility[40-44]. PANI based potentiometric sensors have demonstrated very promising near Nernst sensitivity of around 50-60 mV/pH with good repeatability and stability[33, 41, 45-46]. Polypyrole, Pentacene, and P3HT are also (semi-)conducting polymers, which show decent activity towards pH sensing[47-49].

PEDOT:PSS is the most popular conductive polymer in the organic electronics domain due to its wide range of adjustable conductivities, transparency, modifiable bandgap, printability and biocompatibility[50-53]. PEDOT:PSS is applied to develop pH sensors, which are described in different research works[46, 54-56]. pH sensing is realized by noting the conductivity changes of the PEDOT:PSS layer[57-59]. In recent times, organic compounds are increasingly being used in biosensors[12]. Alizarin is such an abundant, cheap, solution-processable, and biocompatible material choice[60]. Alizarin, basically an organic dye for textile fabrics, is also applied as a staining agent to identify calcium-containing osteocytes in cell cultures and for biosensor development[61-64]. pH activity of the Alizarin material is already reported in previous works[65-67]. Voltammetry based carbon-alizarin composite electrodes are used in pH sensing[68-69]. The carbon-alizarin sensor has shown a linear sensing behavior with a sensitivity in the range of 55 mV/pH and the sensor was equally good in buffered and unbuffered media[70].

Although multiple pH sensing materials and methods are studied, there exists a lack of clarity in elucidating the best fitting one towards a wearable sensor. This work layouts an investigation towards highly reproducible, wearable and significantly sensitive pH sensors

by applying the right combination of the suitable electrochemical sensing method, the right materials, and compatible production techniques. This overview is a combination of own experiments combined with relevant literature sources and leads to an overview on selection criteria for wearable pH sensors. To prove this last point, we have further developed, based upon this selection, a wearable pH sensor on a textile substrate. Integrating pH sensors onto textile substrates meet the requirements of end-user suitability, sensing functionality, and economical feasibility. A limited amount of research has been reported on printed pH sensors on textiles. Further the major concerns regarding a textile pH sensor are their capability to sense pH over a biologically relevant pH range and its hystersis issues in pH cycles[32, 71]. These elements are lacking in the afore reported works and hence this article, apart from being a clear investigative study towards the selection of sensor principle, materials and production technology, also introduces a highly sensitive pH sensor fabricated on a textile substrate that can measure pH in a physiologically relevant range. Textile substrates are desirable due to their compatibility with the human body, breathability, and user convenience[39, 72]. This work investigates three electrochemical organic and conductive polymer based sensor development principles to produce a consistent pH sensor on textiles for wearables. PANI, PEDOT:PSS and Alizarin are the materials of experimental interest here and they are selected for a couple of reasons.

a) Above mentioned materials have previously been investigated for their pH sensing functionality and have shown to be potential ones

b) Those materials are readily available in the research domain and inexpensive for industrial production

c) They are used on some flexible foils, and other textile end applications imply their feasibility in using them in smart textiles[39, 73-74]

d) Chosen functional materials are easily processable; mostly they are proven as printable

e) They are environmentally stable, biocompatible materials

f) These materials are previously reported for antimicrobial properties[75-76]

This work investigates the performance, linearity, sensitivity, and repeatability of these three sensor types based on the experiments performed together with literature knowledge. The first phase of the experiments is set to fabricate these three sensors into foils applying screen printing and ultrasonic spray coating (USSC) for material deposition. Based on sensor wearability, feasibility to produce on textiles, and sensing features along with previously published work, we narrow down the objective to a single sensor that leads to a final printed pH sensor on textiles for health monitoring.

2 Materials and methods

2.1 Theory of the sensor working principles

The functioning of three different sensor principles is considered here. A first one is a conductometric PEDOT:PSS based sensor, a second one is a voltammetric carbon-alizarin sensor, and finally a potentiometric PANI sensor is investigated.

2.1.1 Conductometric PEDOT:PSS based pH sensors

The conductometric pH sensor working is envisaged here based on the resistance changes of the chemistor sensing material upon pH buffer exposure. Resistive readout-based pH sensors are described previously where those works mostly applied microfabrication techniques and allotropes of carbon[16, 77-78]. This work applies PEDOT:PSS as one of the sensing elements where the conductivity modification occurs due to the electrochemical changes induced by the pH of the analyte in the sensor. The electrochemical properties of conjugated conducting polymers are highly dependent on the structure of the polymer film. PEDOT:PSS is ubiquitous in research, widely studied material showing reversible morphological changes towards pH[79-80]. PEDOT:PSS has a redox-active conjugated backbone with multiple redox states. **Figure 1** explains the micro-morphological changes in the PEDOT:PSS layer with respect to pH. When the PEDOT:PSS layer is exposed to acidic pH, it forms an uninterrupted, loose, and porous structure. The PEDOT chains are uniformly distributed on the PSS polymer backbone. The optimized distribution of PEDOT chains ensures the conductive networks within the PEDOT:PSS layer. As the pH changes to alkaline, microstructure of the PEDOT:PSS film transforms from a continuous network to non-continuous clusters. The presence of hydroxide ions leads to the formation of phase separation between PEDOT and PSS. The network of PSS polymer chains surrounds short PEDOT chains, leading to a drop in conductivity. This morphological change in PEDOT:PSS makes it an exciting choice for a conductometric pH sensor. Resistance tracking based pH sensors need the simplest electronic readouts, and such sensor systems do not require a reference electrode for their pH sensing functionality. Upon exposure and drying of the pH buffer on the printed PEDOT:PSS layer, a change in

resistance with respect to its initial resistance is exhibited, which correlates to the pH of buffer dropped on the sensor. This pH values of buffer and resistance change can be plotted in a linear scale.[57-58, 80-81]

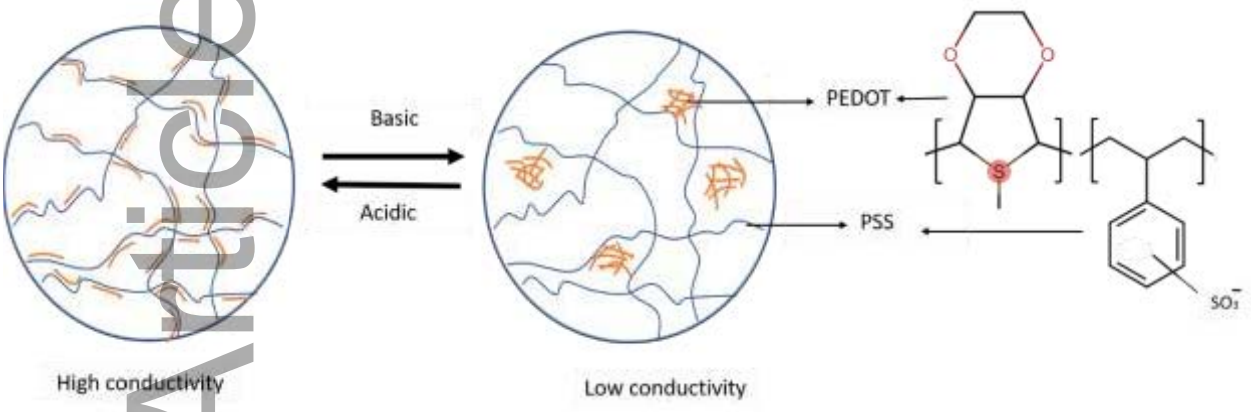

Figure 1 pH induced morphological changes in PEDOT:PSS layer and the chemical structure of PEDOT and PSS

2.1.2 Voltammertric carbon-alizarin based pH sensors

Voltammetry is an electrochemical analytical technique based on the voltage-current relation (voltammogram) of the electrode-solution interface. The technique finds applications in the analyte compositional study, detecting certain electroactive elements or sensing applications. The experimental system consists of a three electrode configuration where the working, reference, and counter electrodes are interfaced together in the test solution. Voltammetry is a notable technique to quantify the solution's pH based on redox peaks that appear on the voltammograms[82-84]. The working electrode is the most vital in the measurement system and there are some of these electrodes reported previously[83-85]. In the proposed work, the working electrode consists of a carbon–alizarin composite where the carbon is an electrically conductive, low density, abundant, and cheap material. Alizarin is an anthraquinone derivative, with hydroxyl groups substituted at the 1 and 2 positions.

pH sensitive quinone moieties present in the Alizarin are the key for the sensor[69-70]. These quinone moieties in the working electrode act as centers of redox reactions with the analyte. The redox reaction in the working electrode is shown as

Alizarin⇌ Anthracene-1,2,9,10-tetrone+nH^{+}+ne^{-}

where n equals 2 hence, it is an $2H^{+}/2e^{-}$ redox process (**figure 2**). These are electrochemically reversible redox reactions. Based on Nernst relation, analytes' pH is linearly correlated to peak potential (E) and it could be written as

$$E = E^{0} - \left(\frac{2{\cdot}303RT}{nF}\right)pH \qquad \text{Equation1}$$

Where E^{0} is the standered potential, R universal gas constant, F is the Faraday constant, T is the temperature and n is the number electrons involved in th reaction.

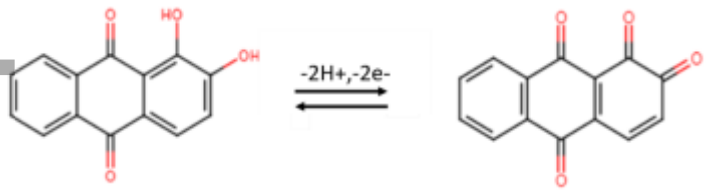

Figure 2 Alizarin molecular changes with changes in pH

2.1.3 Potentiometric graphene/PANI sensor

Potentiometry is a simple technique in electrochemistry to measure the potential difference (across the sensing electrode and reference eectrode immersed in test solution. This technique has been used in multiple sensing platforms, and nowadays, it grabs widespread recognition in wearable sensors[86-87]. The sensor system is comprised of a

working electrode made up of an ion-selective membrane and a reference electrode. A change in the concentration of ions in the bulk sample solution produces variation in the membrane potential. This is measured as an open circuit potential (OCP) between the reference and the working electrode and is served as the readout. In this study, the working electrode is configured in such a way that graphene is modified with a pH sensitive PANI coating. PANI is an intrinsically conductive polymer with semiflexible nature. PANI has pH sensing capabilities due to its multiple redox states and its reversible interconversions of emeraldine base (EB) to emaraldine salt (ES) as illustrated in **figure 3**.

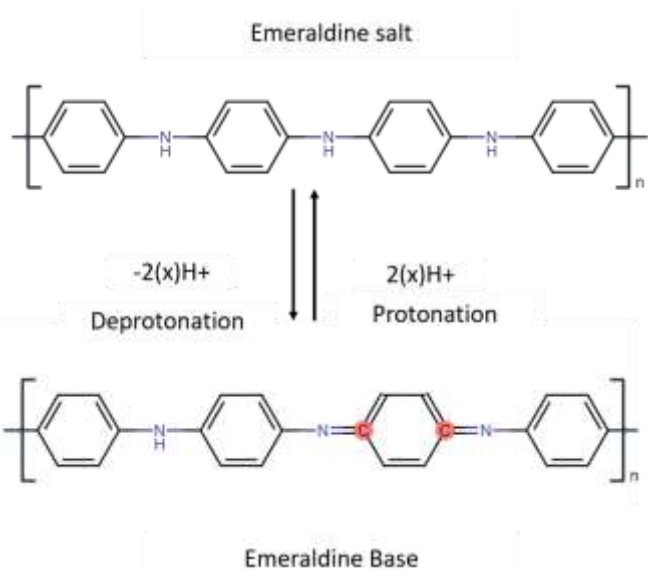

Figure 3 PANI emeraldine protonation and deprotonation

ES and EB moieties of PANI in a test sample environment reaches an electrochemical equilibrium, which leads to an inversely proportional potential generation with respect to the sample pH. Higher pH conditions lead to deprotonation of PANI and causes very low conductivity. This makes the use of PANI alone - difficult for sensors applications[88]. In contrast to PANI, the synergy of graphene-PANI composites (allotropes of carbon with PANI) could enhance its properties in terms of flexibility, electroactivity, conductivity, and

have shown antimicrobial properties[89-90]. Graphene is a 2D nanomaterial with sensational thermal, electrical, chemical, mechanical, and optical properties that are highly desirable for many applications. In a recent study, Lin et al. made a serendipitous discovery that porous graphene can be induced on the polyamide foil with a laser scribing at low power settings[81]. This laser source creates photochemical and photothermal changes on the substrate leading to the formation of 3D porous graphene. As a facile approach to get graphene on flexible substrates, it leads to tremendous applications in wearables[91-92].

2.2 Sensor Fabrication

For the sensor fabrication, this research work applying two different printing/coating technologies. The first one, ultrasonic spray coating (USSC), is a versatile non-impact, large-area solution/dispersion coating technique. The printhead's ultrasonic vibration inducing standing waves on the solution drop leads to its atomization, provides consistent drop size, and a high degree of coating uniformity on 2D and 3D surface. USSC found great importance in high precision thickness (from nanometer scale) and uniform active layer deposition of solar cells, light emitting diodes, sensors, and other functional coating applications, especially in large areas[93-94].

The second technology, screen printing, is a conventional technique categorized as a thick film material deposition method. The setup comprises a fabric screen stretched and attached to a frame, and the unwanted areas of the screen are masked with a suitable emulsion. The functional material in the form of a printing ink is pushed through the unmasked areas of the screen with the help of a rubber squeegee into the substrate. Printed electronics heavily depend on screen printing as it's a simple, long time known

material deposition technique in mass volumes and the compatibility to print a variety of material compositions on different substrates from paper to foil to textiles[95-96].

The work used inhouse prepared Britton-Robinson buffer characterized with a commercial pH meter for the sensor testing.

2.2.1 Conductometric PEDOT:PSS based pH sensor

High conductive grade PEDOT:PSS Clevios PH 1000 from Heraeus, Germany and flexible silver paste from Gwent group are used for sensor fabrication. The sensor fabrication starts with cleaning the PET substrate using isopropanol alcohol together with cleanroom wipes. Then silver paste to form two electrode contacts of the sensor were printed. The electrodes are spaced 5 cm apart on the substrate. These printed silver electrodes are cured at 130 ^{0}C in a box oven for 10 minutes. Followed by this step, a PEDOT:PSS structure was deposited via ultrasonic spray coating. The spray coatable PEDOT:PSS was prepared using a high conductive version of it. Clevios PH1000 PEDOT:PSS is diluted with IPA in the ratio of 1:4. The coating parameters include flow rate of 0.35ml/min and the hot plate temperature to 70 ^{0}C. The multipass PEDOT:PSS layer is deposited with USSC and only the desired area of the sensing area is kept exposed to the coating. Then it is cured at 130 ^{0}C for 10 minutes. Both junctions of PEDOT:PSS to silver are coated with a polydimethylsiloxane elastomer (Sylgard 184) and preceded by a curing step at 70 ^{0}C in a box oven, so that the silver electrodes do not get wet during the testing. The sensor set-up is shown in **figure 4** .

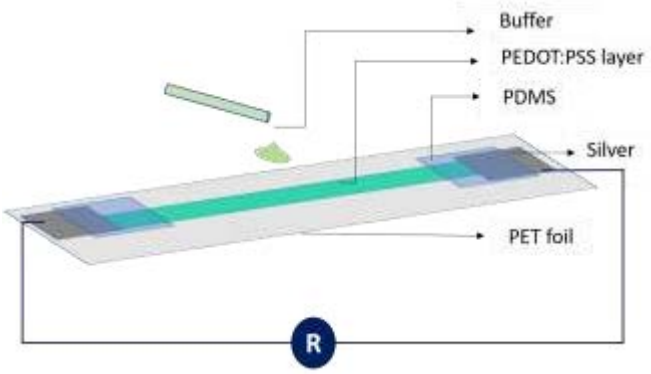

Figure 4 Conductometric type PEDOT:PSS sensor on foils

2.2.2 Voltammertric carbon-alizarin based pH sensor

The working electrode for the sensor is made up of Alizarin ($C_{14}H_8O_4$) and was purchased from Sigma Aldrich and high conductive carbon paste LOCTITE EDAG PF 407A E&C was supplied from Henkel, Belgium. The carbon paste is mixed with Alizarin using a speed mixer (Hauschild model DAC 600.2 VAC-P) at 2500 rpm for 2 min at a fixed weight ratio of 15:1[70]. This prepared paste is screen printed using a predesigned screen on a PET foil and cured at 130 ^{0}C. Followed by this, a layer of silver paste is printed on the tracks and contacts. Leaving the sensing area open, the track is covered with the same polydimethylsiloxane (PDMS) elastomer and followed by curing, as mentioned before. The alizarin based working electrode and voltammetric measurement system is depicted in **figure 5**.

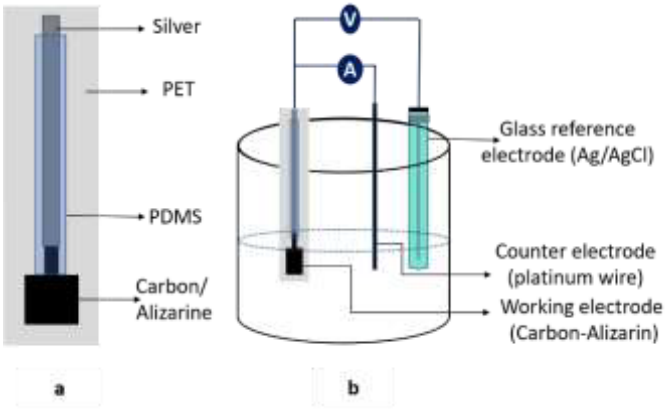

Figure 5 Carbon-alizarin based working electrode (a), The measurement set up of the voltametric measurements (b)

2.2.3 Potentiometric graphene/PANI sensor

Polyaniline emeraldine base (20000 g/mol) from Sigma-Aldrich was dissolved in 99.9% dimethyl sulfoxide (DMSO), resulting in 0.4 wt% PANI-DMSO ink. The ink was homogeneously mixed using a speed mixer and a vortex mixer. Additionally, the ink was filtered using a disposable 'Chromafil GF-100/25 MS' filter with pore size of 1 µm. Kapton substrates are cleaned with solvents, followed by the 3D porous graphene formation on the substrate with the help of a CO2 laser. Laser induction on polyimide sheets has been performed using Universal Laser Systems, VLS2.30 equipped with a wavelength of 10.6 µm pulsed CO2 laser system (25 W). The polyimide sheets `were purchased from Good fellow. A scan rate of 20 cm/s, a laser duty cycle of 30%, and an image density of 1000 ppi were used to obtain a black layer of LIGNs on the polyimide sheets. Then a reference electrode is printed where the salt-bridge based on water-based polymeric ink (Tubicoat from CHT group, Germany) and pottasium chloride salt powder (KCl) was prepared. Tubicoat and KCl are mixed in a weight ratio of 10:1. A silver electrode is screen printed next to the LIG electrode and cured. Then stencil printed the saltbridge on top of the silver electrode and cured at 120 ^{0}C in a box oven for the reference electrode. The sensing area of the porous

graphene is coated with PANI and masked other areas. PANI deposition is made with USSC setting a flow rate of 0.1ml/min and the hot plate at 90 ^{0}C. The sensor was then cured at 150 ^{0}C in inert condition for 10minutes. A thin layer of the polydimethylsiloxane elastomer covered the complete printed area, except the active sensing area and is cured as similar to the previous ones. **Figure 6** represents the build-up of the printed working and reference electrodes and the sensor set up.

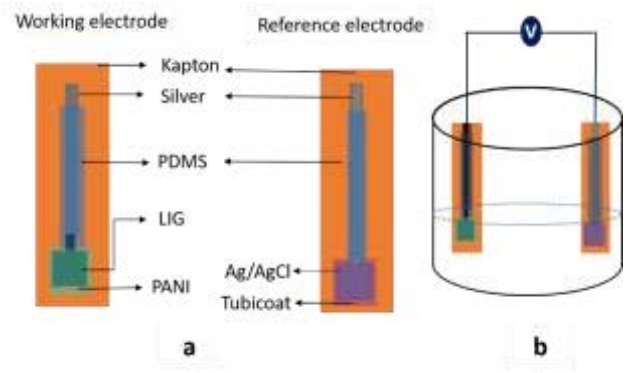

Figure 6 Working electrode and reference electrode structure is shown (A) and the sensing set up used (B).

2.2.4 Textile potentiometric graphene/PANI sensor

The substrate used for the final sensor fabrication is a polyester woven fabric (100% Polyester - washed and fixated - kw11401) from Concordia Textiles (Valmontheim, Belgium) with an average roughness of 6µm. It has shown good printability and flexibility properties and is stable up to 140^{0}C. A layer of insulative ink (Tubicoat MEA, CHT group, Tübingen Germany) is screen printed and cured at 130^{0}C. Carbon and silver paste are screen printed onto the insulative layer to form the conductive electrode and cured at 130 ^{0}C for 10 minutes in a box oven. A salt bridge is stencil printed on the silver electrode and cured as mentioned previously .On the other side of the substrate (not the electode printed

surface), a layer of PDMS is deposited using a bladecoater and is then cured at 70 °C for 20 minutes. The polyaniline ink was spray coated on the carbon electrode and cured as mentioned in the previous section.

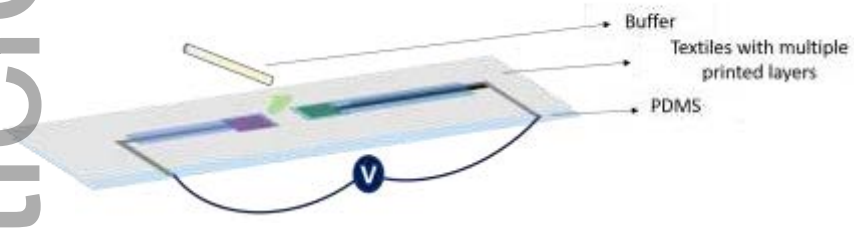

Figure 7 Depiction of potentiometric PANI sensor on textiles

3. Results

3.1 Conductometric PEDOT:PSS based pH sensor

Discrete volumes of buffer solutions with pH values ranging from 4 to 10 are used for the sensor characterization. Once the buffer is dropped on the sensing part, it takes a few minutes to give acceptable responses. To facilitate accurate sensing, the buffer drop on the sensor surface needs to be properly removed. Whereas the pH of the buffer changes from 10 to 4.5, a drop in resistance is observed as it is shown in **figure 8b**. This drop in resistance is attributed to occur from the morphological changes of the PEDOT:PSS upon exposure to buffers of different pH. PEDOT:PSS is an intrinsically conductive polymer and consists of PEDOT and PSS ionomers. The presence of acidic medium improves the PEDOT alignment with PSS, which is attributed to the increased conductivity. This is supplemented in the UV-VIS absorption spectrum of PEDOT: PSS exposed to different pHs shown in **figure 8a**. Relatively lower pH buffer exposures give rise to a broader absorption in the

NIR region, which indicates the presence of bipolarons. This explains the better conductivity of the PEDOT:PSS layer in lower pH exposure. Contrary to this, the basic medium causes the interruption to the PEDOT to PSS charge balance that decreases the density of polarons and bipolarons in the PEDOT chains. The higher pH conditions reduce the bipolarons to polarons (900 nm) and neutral (600nm) species, diminishing the conductivity.

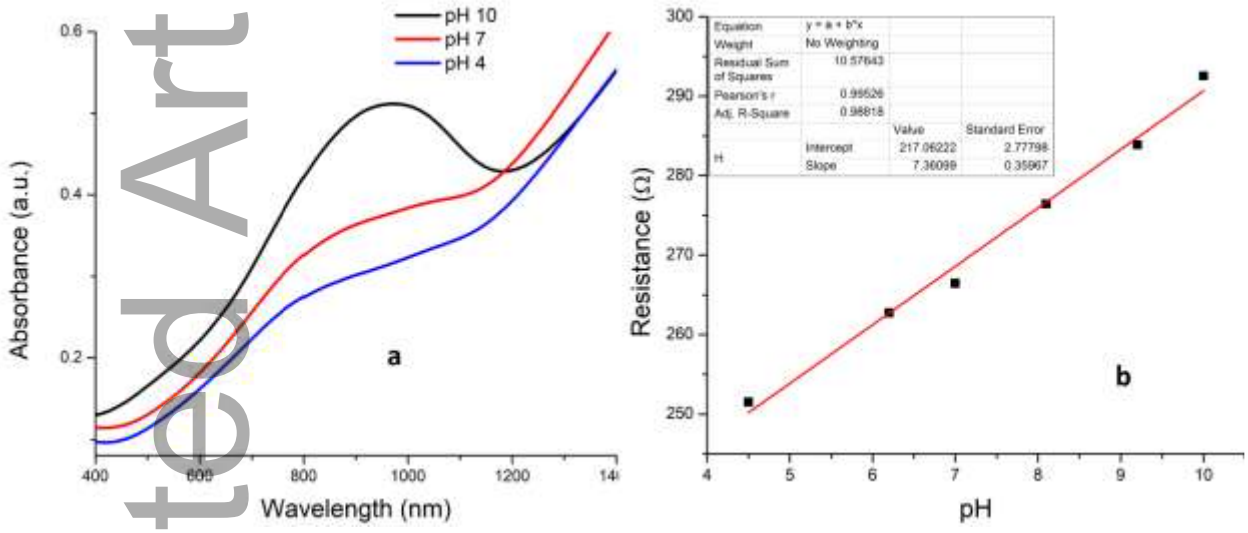

Figure 8 (a) UV visible spectrum of PEDOT:PSS layer dipped in different pH buffers and dried. (b) Resistance changes occur on PEDOT: PSS sensor with different pH.

In order to ensure the repeatability of the measurements, the sensor has undergone for another set of measurements in the reverse order. The repeated measurements as well showed broadly similar plots **(figure 9)**. However, the sensor performance is substantially dominated by the hysteresis nature of the sensor. Since the PEDOT:PSS material is being doped multiple times with the pH buffer during the 1st set of measurements, the sensor is not fully recovered to its initial status during the 2nd set of measurements . Thus the protonation/deprotonation charge exchanges are not fully reversible. Naficy et al. also reported for similar kinds of hysteresis in their PEDOT:PSS based hydrogel pH sensor[58].

Besides this, experiments indicate that the sensor system has different sensitivity in cycle 1 and cycle 2. This inconsistency and offset in sensor performance limits the functionality of the sensor into one-time use applications. Resistance readout principle based printed sensors for wearables are previously reported. Many of them are designed to be for single use (exposure of the body fluid limited to one time), which is adequate for minimal end-uses[77, 97].

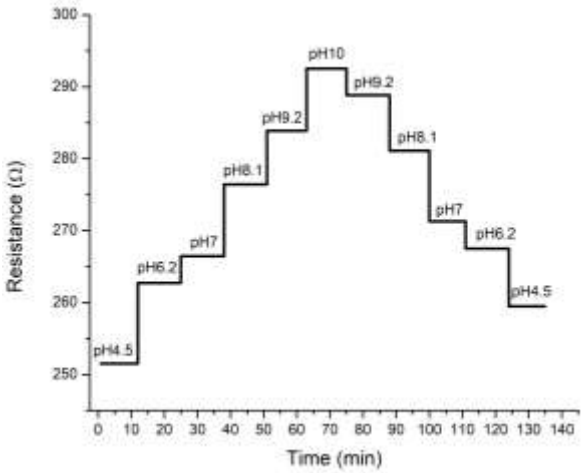

Figure 9 PEDOT:PSS sensor tested for ascending and descending order of pH buffers

3.2 Voltammetric carbon-alizarin based pH sensor

The sensor system has been tested for a range of buffer from pH 4 to 9.5. The sensor in a test solution is scanned with an applied voltage from 0 to 1V and a scan rate of 50mV, a distinct single redox peak is realized in the voltammogram **(figure 11a)**. The voltammogram corresponding to each pH buffer shows a unique current peak. As the buffer's pH goes from acidic to basic, the corresponding voltammogram peak is observed to occur at lower voltages. The shift in peak position is also observed in the UV-VIS absorption

spectra for Alizarin material treated with different pH buffer. **Figure 10** is a clear indication for the changes in the molecular structure of Alizarin in different pH conditions.

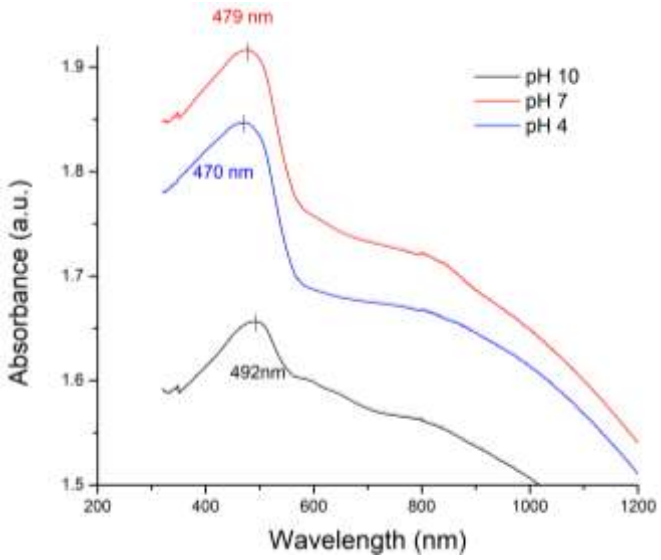

Figure 10 UV-VIS absorption spectrum for alizarin layer exposed to a range of pH buffers.

The peak shifted from 492 nm to 470 nm in response to the treatment of pH 10 and pH 4 solutions. This can be explained as the decrease of the Alizarin's LUMO-HOMO energy gap with increasing pH[98]. In concurrence to this, a shift in the oxidation peaks is observed in the voltammogram to lower values with an increasing pH. The voltage at which the peak is obtained has a linear dependence on the pH of the test solution which can be observed from **figure 11b** and follows the Nernst relation. The sensitivity of the sensor is calculated from the voltammogram measurements as 55 mV/pH and it is in close agreement with the previously reported similar sensors. The sensor has been tested multiple times consecutively for the same buffer to ensure its peaks are not a random occurrence. In **Figure 12a**, the reproducibility of the repetitive measurements are clearly established from the precise alignment of the peak of the voltammogram at the same position.

Moreover, it proves that the number of measurements have no significant influence on sensor performance.

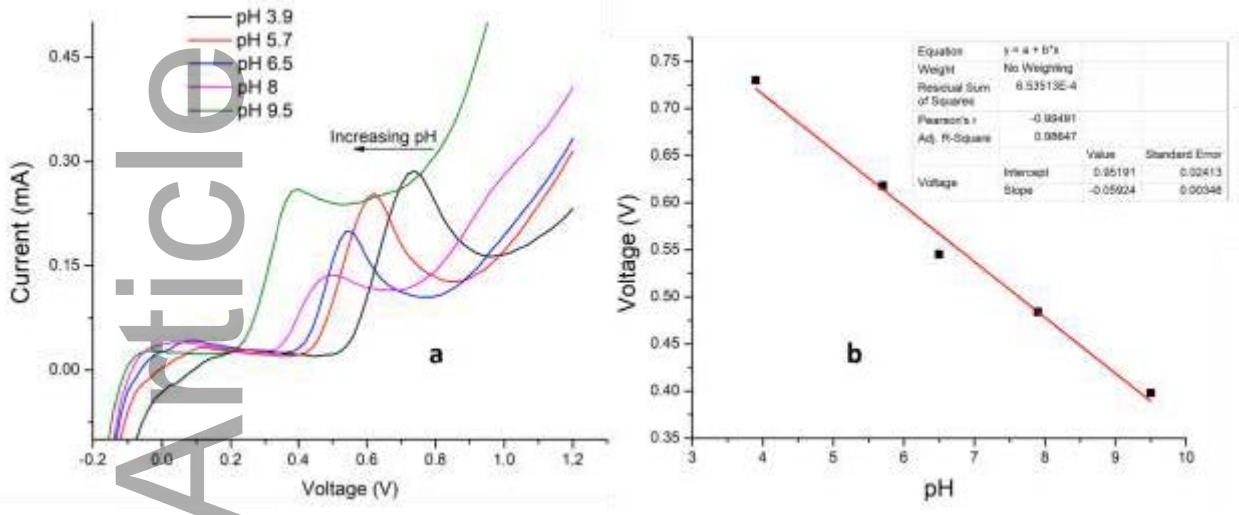

Figure 11 (a) Voltammogram of Alizarin based pH sensor, (b) The peak position in the voltage axis is redrawn against pH

However, the sensor shows shifted peaks for each pH when the measurements are compared between cycles; i.e. sweeping from low to high pH value, over and over again (**figure 12b**). All the 2nd cycles' measurements appeared to have the peak moved slightly to the left in the voltammogram compared to the 1st cycle. Although the voltammograms in the 2nd cycle show a drift to the left, it was not of equal magnitudes for all pH measurements. This may arise due to the memory effect or hysteresis of the sensor after a set of measurements.

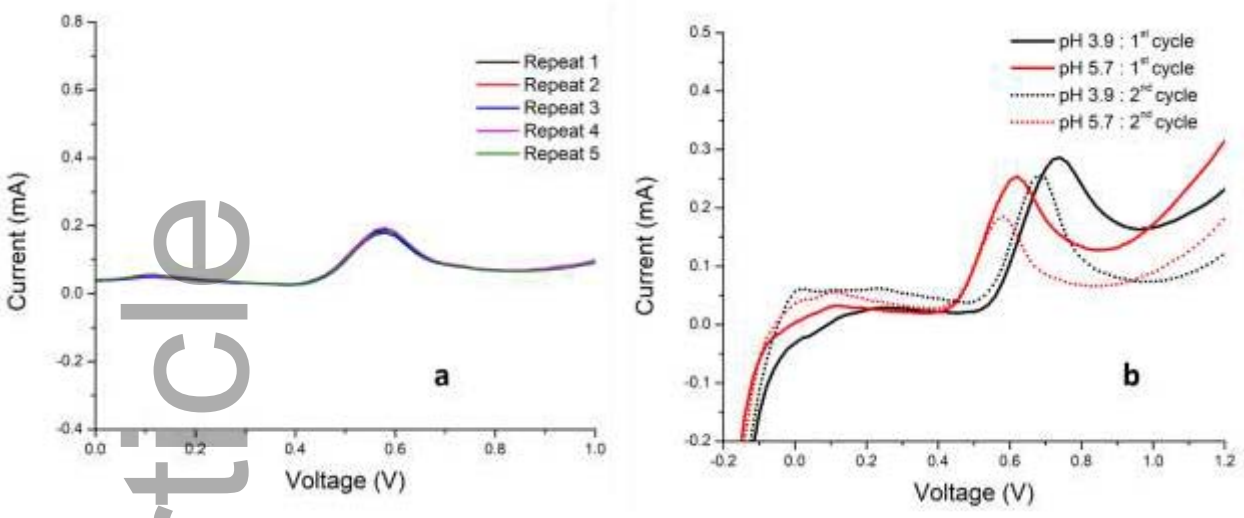

Figure 12 (a) Voltagram of pH 5.7 buffer for five repeated cycles in a row, (b) Voltagram of pH 3.9 and 5.7 buffer in two different cycles

3.3 Potentiometric graphene/PANI sensor

This sensor development initiates with the process to obtain laser induced graphene (LIG) on a polyamide foil. **Figure 13a** shows the SEM images of the porous fibrous structure formation of 3D graphene. The Raman spectrum shown in **Figure 13b** contains D, G and 2D peaks[81, 99]. The D peak at 1342 cm^{-1} indicates the presence of structural edge defects of sp^3 centers in LIG. The G peak and 2D peak are at 1540 and 2680 cm^{-1}, respectively, which represents the existence of sp^2 phases in LIG. The I_D/I_G ratio of 0.34 and I_{2D}/I_G ratio of 0.53 indicate the presence of high degree of sp^2 network and formation of multilayered graphene in LIG[100]. The graphene electrode is modified with a thin layer of spray coated polyaniline.

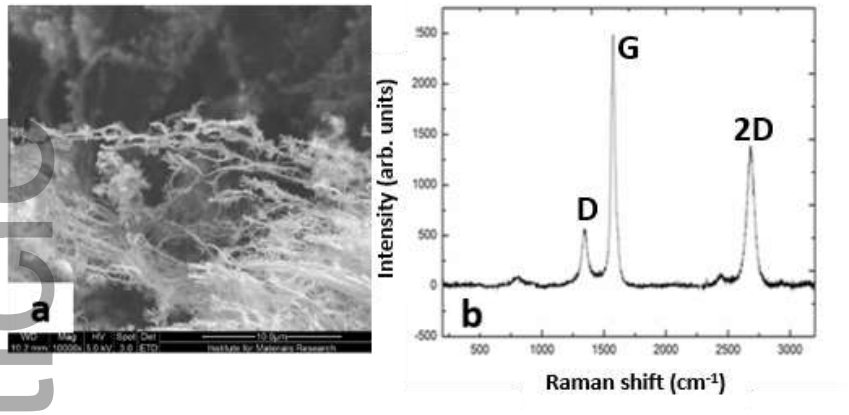

Figure 13 (a) SEM morphology , (b) and Raman spectrum of the laser induced graphene

Potentiometric readings of the sensor are taken in the pH buffer against the Ag/AgCl reference electrode (the sensor readings against standered glass referance elctrode is displayed in figure S5). The PANI coated graphene serves as an ion selective electrode for pH sensing. The H^+ ions can be detected through the protonation and the deprotonation process of PANI, leading to OCP changes against the reference electrode. In the previous section of the voltammetric sensor, a standard glass reference electrode was used to characterize the foil sensors. However, it is not practicable to be in health monitoring end-uses as it is fragile, not possessing a wearability form factor and is an expensive choice. So the work is extended to the fabrication of a solid-state reference electrode into foil applying printing techniques. The reliability of the reference electrode is detrimental to sensor performance and reliability. Many wearable sensors are reported with quasi reference electrodes, but they are not ideal for health monitoring due to cross-sensitivity and short lifetime[101]. This work utilizes solid-state reference electrodes with a polymer based solid-state salt bridge. This type of reference electrode needs a longer time for the initial stabilization than the standard glass reference electrode, where the salt bridge consists of liquid media. The proposed electrode is made up of a printed silver electrode turned into a silver/silver chloride by electrodeposition. To maintain a constant potential, a salt bridge layer is deposited on the silver/silver chloride. The salt bridge layer consisted out of KCl

and a water-based polyurethane formulation. The printed solid-state electrode is measured against the standard reference electrode and shows that the initial measurement of the reference electrode is getting stabilized after 20 minutes of buffering (**figure 14**).

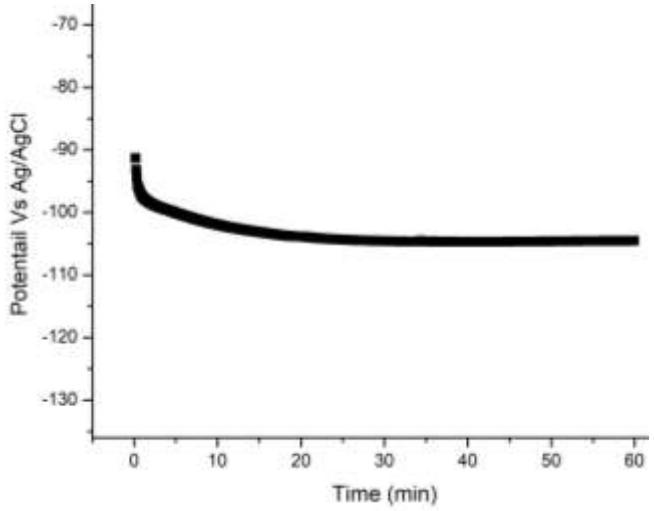

Figure 14 Initial stabilisation of Printed Ag/AgCl reference electrode tested against standard Ag/AgCl reference electrode

The potentimetric PANI sensor readings show a linear relation of open circuit potential (OCP) to pH for a range 4 to 10. Each measurement takes 3 to 4 minutes time to stabilize. The sensor displays a voltage variation of 162 to -155 mV in response to the pH 4 to 10 (**figure 15a**). The readings in the graphs are linear in nature with adj. R^2 value of 0.99 and demonstrate a sensitivity of 53mV/pH. The PANI coated sensor with standard reference electrode and printed reference electrode are compared and they are showing similar performance (supplementary info). The PANI electropolymerized sensor has shown a slightly better sensitivity in the literature compared to this work. However, those production methods are not feasible for low-cost wearable sensors on textiles due to its complicated processing and the involvement of hazardous chemicals[42]. The repeated measurement cycles record identical sensor responses (**figure 15b**), and it proves the ability to read pH accurately.

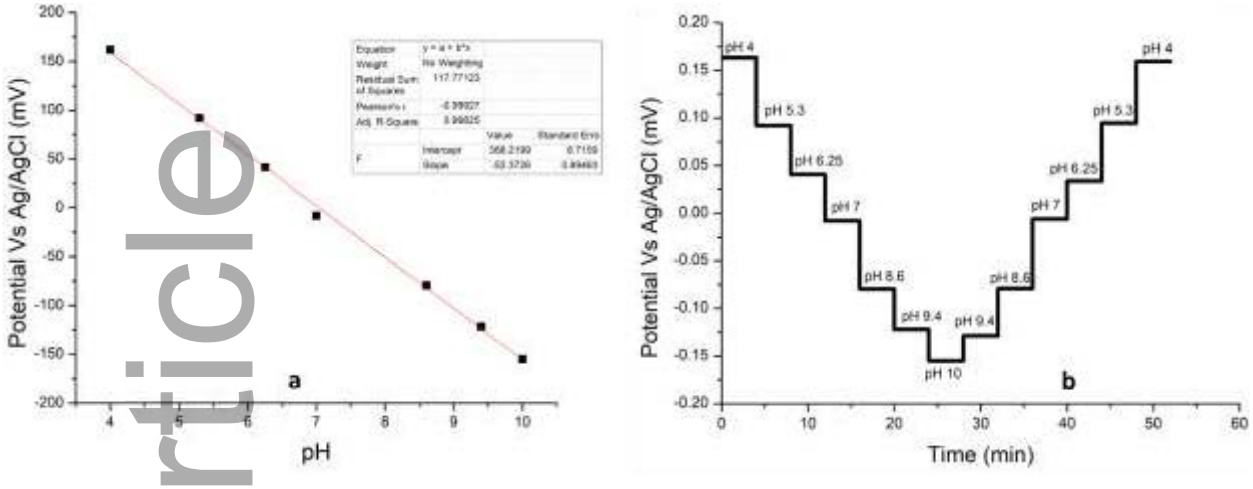

Figure 15 (a) Potentiometric sensor tested for pH 4 to 10, (b) measurement over the repeated cycle

Although there was intense influence of hysteresis found in the other two sensors, the PANI based sensor was not affected by it which is clear from the **figure 15b**. The PANI layer treated with pH buffer is in the states of partially protonated forms of emeraldine base. There are different protonation states and with the low pH (acidic) buffer, a higher protonation is induced, which reduces the peak height at 630nm of UV-VIS absorption spectrum (**figure 16**). Further, at 900 nm, a higher amount of polarons are found in the films treated with lower pH buffer[102]. However there are no changes noticed in the peak position in the range of pH 4 to 10.

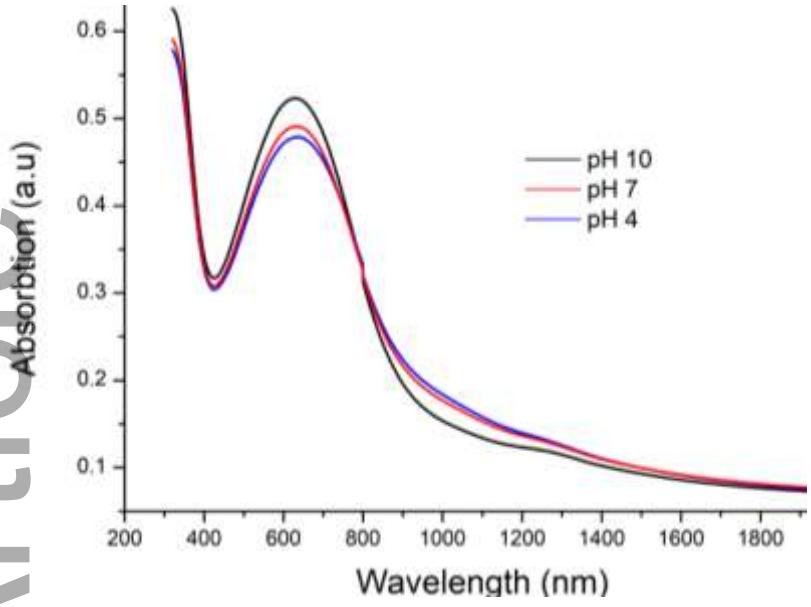

Figure 16 UV-VIS absorption spectrum for PANI layer treated in different pH buffer

3.4 A sensing approach and property comparison to achieve textile-based pH sensors

pH sensor development for textile and wearable applications demands specific classic prerequisites, being of great importance. Tehrani et al. listed some of them, including ease of manufacturing, availability of the materials for fabrication, high sensitivity, stability, and fast response time[103]. In the context of a textile based sensor, it has to meet wearability priorities along with its sensing functionalities. As the sensor is being used in guiding medical diagnostics, sensor features such as accuracy, repeatability, and stability are indispensable. The printability, flexibility, bendability, biocompatibility, and feasibility to fabricate sensors into textile facilitates to encompass highly pertinent prospects of non-invasive health monitoring through end-user convenience at low cost. Some of the significant sensor characteristics are investigated in this work. However, along with this work, the previously reported works are taken into account to further develop sensor on textiles.

The fabricated sensors (**in figure S1**) mostly used printing and coating based production methods, which is comparatively less complex than conventional approaches for pH sensor production. The carbon-alizarin composit ink is highly viscous and possess shear thinning behaviour which facilitated the material deposition with screen printing. The printed functional layer shown adequate conductivity and uniformity. Similarly, PANI formulation have low visocity which can be adjusted with respective solvents. The ink attributes matched for inkjet printing and USSC deposition and tiny atomised droplet deposition of USSC ensured high quality and uniform material depsition of PANI functional layers[104-105]. Different from other two materials, PEDOT: PSS is reported to be compatible for printing with a range of printing techniques from screen printing[106], gravure printing[107], inkjet printng[108], flexographic printing[109] and many coaing techniques. The viscosity adjusted formulation of PEDOT:PSS layer deposited with optimised layer thickness using USSC shown to be excellent in transperency and conductivity properties. The reference eletrode printing is also cmpletely carried out with printing tehniques. Yet PEDOT:PSS based conductometric sensors do not need a reference electrode, and it makes the sensor fabrication route simple with respect to the other two sensor principles.

Materials used for sensor fabrication are readily available in the commercial domain and previously applied to produce devices on textiles. Biocompatibility in terms of cytotoxicity is investigated for PANI and PEDOT:PSS in different works and was concluded as non-toxic[43, 110]. Alizarin (Madder) is used as an antimicrobial agent in skincare products and in wound cleaning[60]. Those reports counted them as biocompatible and eligible for bioelectronics applications. In the context of a simplified sensor readout for wearables, the passive resistive and potential measurements posseses advantages whereas voltammetry

is an active method that adds some complexities into it. All of these properties are summarized in **figure 17**.

The sensitivity of the sensors are considered for the range from pH 4-10. Voltammetric and potentiometric sensors have sensitivity of 55 and 53 mV in this work and are concurring with literature reported values[42, 70]. The conductometric sensor shown a sensitivity of 7.5 Ω/pH in the range of 4.5 to 10. The linearity of all three sensors was decent, and PANI and alizarin-based sensors displayed a correlation coefficient of 0.99. The potentiometric sensor readings repeatability confirms an excellent agreement between the measurement cycles; however, the other sensors have demonstrated poor performance, mostly due to the memory effect and the functional material dissolvability in buffer. As shown in **figure S2**, multiple sensors are tested within the sensor type and show quite similar sensing behaviour for all sensor types. The response time of the PEDOT:PSS sensor was comparatively longer as the sensor has to be dried after getting wet in order to get the intended reading. Accuracy of the conductometric PEDOT:PSS sensor in real life measurements is under suspicion as the sensor structure has to be uniformly wet, and its dryness is related to the function of the pH measurements. Besides, the measurement reproducibility is inferior for the conductometric and voltammetric sensors. However, the PANI sensor demonstrated excellent sensing characteristics, and the readings are repeatable. Stability of the sensor readings are another relevant aspect and PANI based sensors show 48 hours of continuous testing without significant stability drops[111]. Conversely, the alizarin from the voltammetric sensor was found slightly dissolving in

alkaline buffers. Similarly longer time exposure of PEDOT: PSS layer to buffer media can lead to its deterioration due to its dispersibility in water.

Bendability, flexibility, and stretchability of the sensor are predominant attributes related to its wearability function. All the three sensors were rolled in a cylindrical shape with a diameter of ~ 1.5 cm as shown in figure S3 a&b. This step was repeated for ten times and subsequently, the sensors were tested. Whereas the potentiometric and voltammetric sensor readings (in figure S4 b&c) have not shown any significant changes from the previous measurements indicating their robustness. the PEDOT:PSS sensors show 5% resistance change in the sensor readings from its initial resistance. The PEDOT:PSS based pH sensor has constraints in exhibiting bending or flexing attributes as its resistance would change in such instances that can influence the pH sensor reading. Wearability features of Alizarin are not cross-examined further as it is known as a textile dye for a long time. The potentiometric PANI sensor's wearability attributes and mechanical properties are also reported for sensing applications in other literature sources[112-113]. These sensors can be flexible and bendable in a relatively large extent[45]. Rahimi et al. demonstrated the PANI sensor on foil in a serpentine design as stretchable[105]. Stempien et al. has shown the performance of the printed PANI layer on textiles and its robustness to washing and mechanical flexing tests[114]. Different studies investigated the selectivity of the PANI based sensor through the influence from the ionic presence on pH sensing. Those studies concluded that no significant impact is found due to the presence of ions like K, Na, which enhances the functionality of the sensor for wearable applications[46, 113]. Temperature is another relevent factor to be considered for pH sensing, however for the on-body

measurements, they are relatively less influential as the body temperatre remains more or less constant.

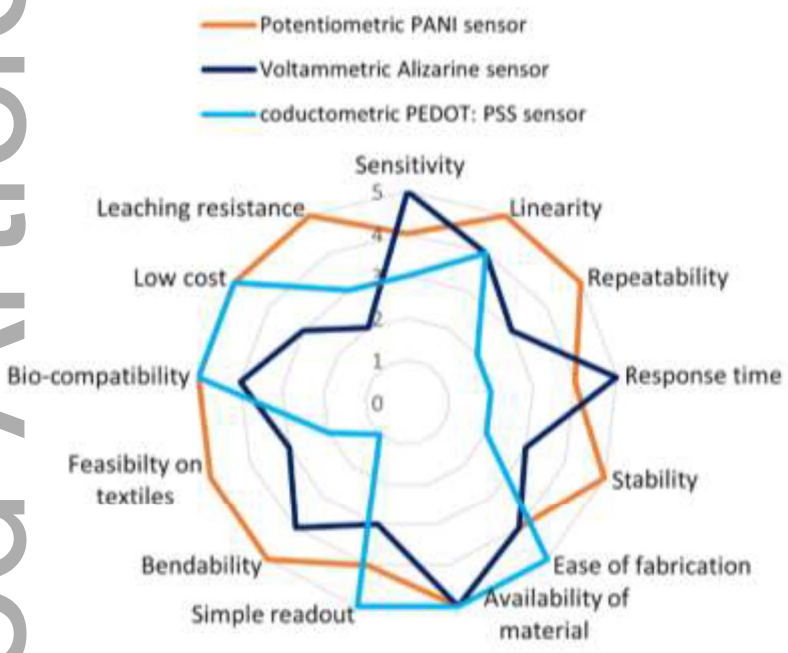

Figure 17 Radar plot to evaluate the three pH sensors discussed in the work based on the results of the work and literature

After a comprehensive analysis of multiple aspects from fabrication, sensor functioning, and wearability features, the PANI-based sensor showed clear advantage over other sensors discussed here. The radar plot also points out the wearability requirements and bioelectronics stipulates could be well addressed with a PANI potentiometric sensor.

3.5 A textile-based potentiometric pH sensor based on carbon/PANI together with a printed reference electrode

Sensor fabrication on textile substrates is one of the noteworthy aspects and an essential objective of this work. The previous section described a detailed screening and selection of

best performing pH sensors. Here, we present the development of a solid-state textile potentiometric printed pH sensor intended for wearable health tracking applications. In contrast to traditional biomedical sensing systems, the textile sensor must meet very stringent requirements. Through setting proper screening measures, here we decided to go with potentiometric pH sensor on textile fabrication. Instead of LIG, carbon is printed on the textile substrate as LIG formation on textiles is hassle, however some new researches show that there are possibilities to achieve LIG on textiles[115-116]. Here the sensor is tested in slightly different conditions as compared to previously mentioned ones. As the sensor needs to address biofluid volumes in microliter ranges, it is designed for such a range of volumes. Here the pH buffer is dropped on top of the electrodes with a few tens of microliter and it is found enough to make good measurements. The spacing between the working and reference electrode could be reduced further, which will result in a threshold volume of the test fluid that can be even reduced.

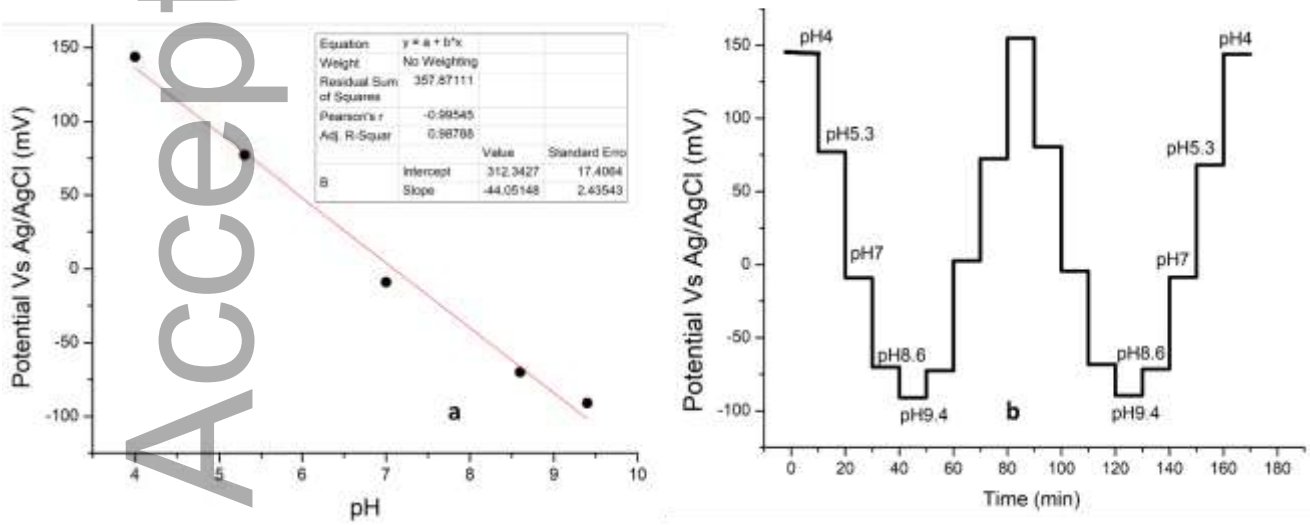

Figure 18 (a) pH sensor on textile tested for the range pH 4 to 10, (b) sensor tested for repeatability

The pH buffer solution is dropped onto the textile sensor such that it connects both electrodes. **Figure 18a** displays the OCP variations with respect to variations in the pH of

the buffer solution. The textile sensor has shown Nernestian sensitivity of 45mV/pH, which is well agreed with the foil made sensor in this work. The sensor measurement readings demonstrate a linear transfer function characteristics with a correlation coefficient of 0.99 over a physiologically significant pH range. The sensor measurement plot (**figure 18b**) shows that the sensor output is substantially the same for increasing and decreasing pH solutions steps in the 4–9.5 pH range. The sensor has been examined multiple times to ensure the repeatability and measured a maximum error of 2.9mV. This confirmes the low error tolerance of pH measurement (~±0.1 pH) which can offer competitive wound monitoring . The pH of the wound varies between pH 4.5 and 8.5 while transiting through the wound healing stages. A freshly formed wound has a pH between 7.4. An abrupt change in the pH can be an indicator of infections. A consistently observed high pH value indicates the chronicity of the wound[7]. Although the sensor has some tolerance in the measurements, the healing status and chronicity could be followed. The sensor readings have shown an overall consistency in its OCP to pH relation in recurring measurements. Yet, there are slight variations in the measurement cycles, and it could be arising from systematic errors. This can mainly occur from the residues left behind on the textiles from previous pH buffer solutions. Also, the quick drying of a few microliter volume of dropped solution can lead to measurement errors.The sensor is also tested for a longer duration, where the sensor is kept in measurements for a time period of 1 hour. The sensor is found to be stable throughout and the readings were stable over time (**figure 19**).

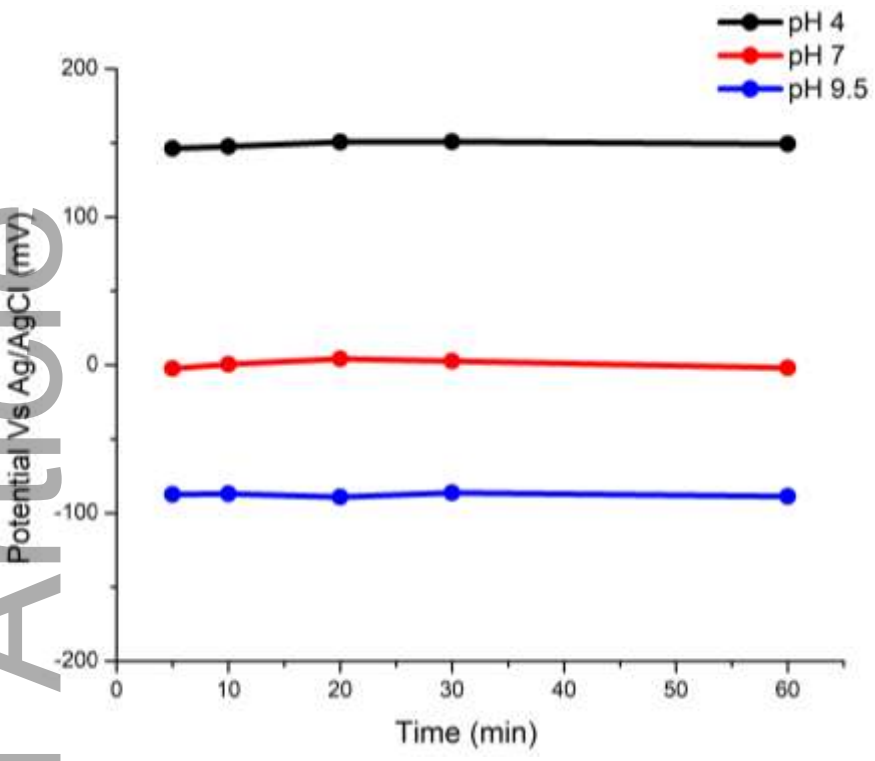

Figure 19 Stability test for textile pH sensor with three different buffer solutions

4 Conclusions

There are a considerable number of pH sensors reported in the literature for health monitoring so far. However, most of them are fabricated on foils applying expensive microfabrication, have limited range, inferior sensitivity, and lack repeatability. There are also difficulties in choosing the right material and sensing technology to be incorporated in wearables. This work explores the organic and polymeric sensing materials as they are found to be engaging in health monitoring due to their exceptional sensing, wearability, biocompatibility and processability properties. Besides that, the sensor is opted to be fabricated on textile substrates due to its ubiquitous wearable nature. This study makes an initial assortment of the most feasible sensor for such applications based on literature. A conductometric PEDOT:PSS sensor, a carbon-alizarin voltammetric sensor and a PANI

potentiometric sensor are experimentally investigated in terms of fabrication with printing techniques, sensing performance, and repeatability. According to the first phase of experimental results and literature background, the PANI-based potentiometric sensor is the most optimal choice towards the objective of the work, among the three different sensor materials and principles investigated. This work also utilises simple printing techniques for pH sensor fabrication which can be applied on foils and textiles. The printed PANI based pH sensor on textiles shows to be promising for a physiologically relevant range of pH values ranging from 4 to 9.5, has a good sensitivity of 45mV/pH, and an excellent repeatability. The selection of textiles and polymer based sensing materials enables wearability. Further, printing and coating techniques together with cheaper compatible materials ensure a more economical large scale production possibility of the wearable sensors. This work strongly asserts economicaly viable pH sensor into more wearable and disposable health monitoring applications which helps to realise an intelligent and portable health management system.

Author Contribution:

Author Contribution: M. Jose, W. Deferme and R. Thoelen conceptualised the work. S.K. Mylavarapu, M. Jose and J. Machiels prepared inks. S.K. Bikkarolla prepared laser induced graphene and K. J. Sankaran characterized the graphene film. M. Jose did the sensor fabrication, testing and other necessary characterisations. A. Hardy And J. McLaughlin aided in interpreting the results and M. Jose prepared manuscript. W. Deferme guided the whole work. All authors discussed the results and commented on the manuscript.

References

1. Czarnowski, D.; Górski, J., Sweat ammonia excretion during submaximal cycling exercise. *J Appl Physiol (1985)* **1991,** *70* (1), 371-374.
2. Patterson , M.; Galloway, S.; Nimmo, M., Variations in Regional Sweat Composition in Normal Human Males. *Experimental Physiology* **2000,** *85*, 869-875.
3. Coyle, S.; Morris, D.; Lau, K. T.; Diamond, D.; Taccini, N.; Costanzo, D.; Salvo, P.; Francesco, F. D.; Trivella, M. G.; Porchet, J. A.; Luprano, J. In *Textile sensors to measure sweat pH and sweat-rate during exercise*, 2009 3rd International Conference on Pervasive Computing Technologies for Healthcare, 1-3 April 2009; 2009; pp 1-6.
4. Yoshida, S.; Miyake, T.; Yamamoto, S.; Furukawa, S.; Niiya, T.; Senba, H.; Kanzaki, S.; Yoshida, O.; Ishihara, T.; Koizumi, M.; Hirooka, M.; Kumagi, T.; Abe, M.; Kitai, K.; Matsuura, B.; Hiasa, Y., Relationship between urine pH and abnormal glucose tolerance in a community-based study. *J Diabetes Investig* **2018,** *9* (4), 769-775.
5. Sun, A.; Phelps, T.; Yao, C.; Venkatesh, A. G.; Conrad, D. J.; Hall, D. A., Smartphone-Based pH Sensor for Home Monitoring of Pulmonary Exacerbations in Cystic Fibrosis. *Sensors (Basel, Switzerland)* **2017,** *17*.
6. Gosain, A.; DiPietro, L. A., Aging and Wound Healing. *World Journal of Surgery* **2004,** *28* (3), 321-326.
7. Schneider, L. A.; Korber, A.; Grabbe, S.; Dissemond, J., Influence of pH on wound-healing: a new perspective for wound-therapy? *Archives of Dermatological Research* **2007,** *298* (9), 413-420.
8. Kumar, P.; Honnegowda, T. M., Effect of limited access dressing on surface pH of chronic wounds. *Plastic and Aesthetic Research* **2015,** *2*, 257-260.
9. AS, B. *Novel Biomaterial for Improved and Cost-efficient Wound Healing*; Norway, 2015.
10. Percival, S. L.; McCarty, S.; Hunt, J. A.; Woods, E. J., The effects of pH on wound healing, biofilms, and antimicrobial efficacy. *Wound Repair and Regeneration* **2014,** *22* (2), 174-186.
11. Gethin, G. In *The significance of surface pH in chronic wounds*, 2007.
12. Sokolov, A. N.; Roberts, M. E.; Bao, Z., Fabrication of low-cost electronic biosensors. *Materials Today* **2009,** *12* (9), 12-20.
13. Sörensen, S. P. L., Über die Messung und Bedeutung der Wasserstoffionen-konzentration bei biologischen Prozessen. *Ergebnisse der Physiologie* **1912,** *12* (1), 393-532.
14. Marczewska, B.; Marczewski, K., First Glass Electrode and its Creators F. Haber and Z. Klemensiewicz@ On 100th Anniversary. *Zeitschrift für Physikalische Chemie* **2010,** *224*, 795 - 799.
15. Lian, Y.; Zhang, W.; Ding, L.; Zhang, X.; Zhang, Y.; Wang, X.-d., Chapter 8 - Nanomaterials for Intracellular pH Sensing and Imaging. In *Novel Nanomaterials for Biomedical, Environmental and Energy Applications*, Wang, X.; Chen, X., Eds. Elsevier: 2019; pp 241-273.
16. Lei, N.; Li, P.; Xue, W.; Xu, J., Simple graphene chemiresistors as pH sensors: fabrication and characterization. *Measurement Science and Technology* **2011,** *22* (10), 107002.
17. Baldini, F., Critical review of pH sensing with optical fibers. *Proceedings of SPIE - The International Society for Optical Engineering* **1999,** *3540*.
18. Głab, S.; Hulanicki, A.; Edwall, G.; Ingman, F., Metal-Metal Oxide and Metal Oxide Electrodes as pH Sensors. *Critical Reviews in Analytical Chemistry* **1989,** *21* (1), 29-47.
19. Manjakkal, L.; Szwagierczak, D.; Dahiya, R., Metal oxides based electrochemical pH sensors: Current progress and future perspectives. *Progress in Materials Science* **2020,** *109*, 100635.
20. Prats-Alfonso, E.; Abad, L.; Casañ-Pastor, N.; Gonzalo-Ruiz, J.; Baldrich, E., Iridium oxide pH sensor for biomedical applications. Case urea–urease in real urine samples. *Biosensors and Bioelectronics* **2013,** *39* (1), 163-169.
21. Simić, M.; Manjakkal, L.; Zaraska, K.; Stojanović, G. M.; Dahiya, R., TiO₂-Based Thick Film pH Sensor. *IEEE Sensors Journal* **2017,** *17* (2), 248-255.

22. Tanumihardja, E.; Olthuis, W.; Van den Berg, A., Ruthenium Oxide Nanorods as Potentiometric pH Sensor for Organs-On-Chip Purposes. *Sensors* **2018,** *18* (9), 2901.
23. Fu, Y.; Pan, J.; Tsou, K.; Cheng, Y., A Flexible WO₃-Based pH Sensor Array for 2-D pH Monitoring Using CPLoP Technique. *IEEE Electron Device Letters* **2018,** *39* (6), 881-884.
24. Sharma, P.; Bhati, V. S.; Kumar, M.; Sharma, R.; Mukhiya, R.; Awasthi, K.; Kumar, M., Development of ZnO nanostructure film for pH sensing application. *Applied Physics A* **2020,** *126* (4), 284.
25. Yilbas, B. S.; Al-Sharafi, A.; Ali, H., Chapter 3 - Surfaces for Self-Cleaning. In *Self-Cleaning of Surfaces and Water Droplet Mobility*, Yilbas, B. S.; Al-Sharafi, A.; Ali, H., Eds. Elsevier: 2019; pp 45-98.
26. Yang, Z.; Pang, Y.; Han, X.-l.; Yang, Y.; Ling, J.; Jian, M.; Zhang, Y.; Yang, Y.; Ren, T.-L., Graphene Textile Strain Sensor with Negative Resistance Variation for Human Motion Detection. *ACS Nano* **2018,** *12* (9), 9134-9141.
27. Sun, F.; Tian, M.; Sun, X.; Xu, T.; Liu, X.; Zhu, S.; Zhang, X.; Qu, L., Stretchable Conductive Fibers of Ultrahigh Tensile Strain and Stable Conductance Enabled by a Worm-Shaped Graphene Microlayer. *Nano Letters* **2019,** *19* (9), 6592-6599.
28. He, X.; Yang, S.; Pei, Q.; Song, Y.; Liu, C.; Xu, T.; Zhang, X., Integrated Smart Janus Textile Bands for Self-Pumping Sweat Sampling and Analysis. *ACS Sensors* **2020,** *5* (6), 1548-1554.
29. Hu, X.; Tian, M.; Xu, T.; Sun, X.; Sun, B.; Sun, C.; Liu, X.; Zhang, X.; Qu, L., Multiscale Disordered Porous Fibers for Self-Sensing and Self-Cooling Integrated Smart Sportswear. *ACS Nano* **2020,** *14* (1), 559-567.
30. Dai, B.; Li, K.; Shi, L.; Wan, X.; Liu, X.; Zhang, F.; Jiang, L.; Wang, S., Bioinspired Janus Textile with Conical Micropores for Human Body Moisture and Thermal Management. *Advanced Materials* **2019,** *31* (41), 1904113.
31. Shim, E., 2 - Coating and laminating processes and techniques for textiles. In *Smart Textile Coatings and Laminates (Second Edition)*, Smith, W. C., Ed. Woodhead Publishing: 2019; pp 11-45.
32. Manjakkal, L.; Dang, W.; Yogeswaran, N.; Dahiya, R., Textile-Based Potentiometric Electrochemical pH Sensor for Wearable Applications. *Biosensors* **2019,** *9* (1), 14.
33. Yoon, J. H.; Hong, S. B.; Yun, S.-O.; Lee, S. J.; Lee, T. J.; Lee, K. G.; Choi, B. G., High performance flexible pH sensor based on polyaniline nanopillar array electrode. *Journal of Colloid and Interface Science* **2017,** *490*, 53-58.
34. Kurzweil, P., Metal Oxides and Ion-Exchanging Surfaces as pH Sensors in Liquids: State-of-the-Art and Outlook. *Sensors* **2009,** *9* (6), 4955-4985.
35. Alam, A. U.; Qin, Y.; Nambiar, S.; Yeow, J. T. W.; Howlader, M. M. R.; Hu, N.-X.; Deen, M. J., Polymers and organic materials-based pH sensors for healthcare applications. *Progress in Materials Science* **2018,** *96*, 174-216.
36. Su, W.; Xu, J.; Ding, X., An Electrochemical pH Sensor Based on the Amino-Functionalized Graphene and Polyaniline Composite Film. *IEEE Transactions on NanoBioscience* **2016,** *15* (8), 812-819.
37. Grancarić, A. M.; Jerković, I.; Koncar, V.; Cochrane, C.; Kelly, F. M.; Soulat, D.; Legrand, X., Conductive polymers for smart textile applications. *Journal of Industrial Textiles* **2017,** *48* (3), 612-642.
38. Nambiar, S.; Yeow, J. T. W., Conductive polymer-based sensors for biomedical applications. *Biosensors and Bioelectronics* **2011,** *26* (5), 1825-1832.
39. Ismar, E.; Kurşun Bahadir, S.; Kalaoglu, F.; Koncar, V., Futuristic Clothes: Electronic Textiles and Wearable Technologies. *Global Challenges* **2020,** *4* (7), 1900092.
40. Crowley, K.; Smyth, M. R.; Killard, A. J.; Morrin, A., Printing polyaniline for sensor applications. *Chemical Papers* **2013,** *67* (8), 771-780.
41. Sen, T.; Mishra, S.; Shimpi, N. G., Synthesis and sensing applications of polyaniline nanocomposites: a review. *RSC Advances* **2016,** *6* (48), 42196-42222.

42. Rahimi, R.; Ochoa, M.; Parupudi, T.; Zhao, X.; Yazdi, I. K.; Dokmeci, M. R.; Tamayol, A.; Khademhosseini, A.; Ziaie, B., A low-cost flexible pH sensor array for wound assessment. *Sensors and Actuators B: Chemical* **2016,** *229*, 609-617.
43. Humpolíček, P.; Kašpárková, V.; Pacherník, J.; Stejskal, J.; Bober, P.; Capáková, Z.; Radaszkiewicz, K. A.; Junkar, I.; Lehocký, M., The biocompatibility of polyaniline and polypyrrole: A comparative study of their cytotoxicity, embryotoxicity and impurity profile. *Materials Science and Engineering: C* **2018,** *91*, 303-310.
44. Yue, J.; Epstein, A. J.; Zhong, Z.; Gallagher, P. K.; Macdiarmid, A. G., Thermal stabilities of polyanilines. *Synthetic Metals* **1991,** *41* (1), 765-768.
45. Li, Y.; Mao, Y.; Xiao, C.; Xu, X.; Li, X., Flexible pH sensor based on a conductive PANI membrane for pH monitoring. *RSC Advances* **2020,** *10* (1), 21-28.
46. Smith, R.; Ward, N.; Varcoe, J.; Crean, C.; Hingley-Wilson, S., *WS.4 - Wearable monitoring of wound pH through a flexible, fibre- based pH sensor*. 2018; p 83-84.
47. Prissanaroon-Ouajai, W.; Pigram, P. J.; Jones, R.; Sirivat, A., A sensitive and highly stable polypyrrole-based pH sensor with hydroquinone monosulfonate and oxalate co-doping. *Sensors and Actuators B: Chemical* **2009,** *138* (2), 504-511.
48. Loi, A.; Manunza, I.; Bonfiglio, A., Flexible, organic, ion-sensitive field-effect transistor. *Applied Physics Letters* **2005,** *86*, 103512-103512.
49. Bartic, C.; Palan, B.; Campitelli, A.; Borghs, G., Monitoring pH with organic-based field-effect transistors. *Sensors and Actuators B: Chemical* **2002,** *83* (1), 115-122.
50. Louwet, F.; Groenendaal, L.; Dhaen, J.; Manca, J.; Van Luppen, J.; Verdonck, E.; Leenders, L., PEDOT/PSS: synthesis, characterization, properties and applications. *Synthetic Metals* **2003,** *135-136*, 115-117.
51. Wen, Y.; Xu, J., Scientific Importance of Water-Processable PEDOT–PSS and Preparation, Challenge and New Application in Sensors of Its Film Electrode: A Review. *Journal of Polymer Science Part A: Polymer Chemistry* **2017,** *55* (7), 1121-1150.
52. Case study: PEDOT:PSS. In *Electronic Structure of Organic Semiconductors*, Morgan & Claypool Publishers: 2018; pp 9-1-9-15.
53. Sultana, N.; Chang, H. C.; Jefferson, S.; Daniels, D. E., Application of conductive poly(3,4-ethylenedioxythiophene):poly(styrenesulfonate) (PEDOT:PSS) polymers in potential biomedical engineering. *Journal of Pharmaceutical Investigation* **2020,** *50* (5), 437-444.
54. Reid, D. O.; Smith, R. E.; Garcia-Torres, J.; Watts, J. F.; Crean, C., Solvent Treatment of Wet-Spun PEDOT: PSS Fibers for Fiber-Based Wearable pH Sensing. *Sensors* **2019,** *19* (19), 4213.
55. Mariani, F.; Gualandi, I.; Tessarolo, M.; Fraboni, B.; Scavetta, E., PEDOT: Dye-Based, Flexible Organic Electrochemical Transistor for Highly Sensitive pH Monitoring. *ACS applied materials & interfaces* **2018,** *10*.
56. Kirchan, A. E.; Kim, K.; Steward, M. K.; Choi, S. In *A PEDOT:PSS-based organic electrochemical transistor with a novel double-in-plane gate electrode for pH sensing application*, 2017 19th International Conference on Solid-State Sensors, Actuators and Microsystems (TRANSDUCERS), 18-22 June 2017; 2017; pp 214-217.
57. Su, S.; Hua, M.-Y.; Cheng, S.; Juan, T.; Shih, M.; Yang, C.-M.; Lai, C.-S., *PEDOT/PSS Membrane on Flexible Substrate for Conductometric pH Sensor Study*. 2012.
58. Naficy, S.; Spinks, G. M.; Wallace, G. G., Thin, Tough, pH-Sensitive Hydrogel Films with Rapid Load Recovery. *ACS applied materials & interfaces* **2014,** *6* (6), 4109-4114.
59. Mariani, F.; Gualandi, I.; Tonelli, D.; Decataldo, F.; Possanzini, L.; Fraboni, B.; Scavetta, E., Design of an electrochemically gated organic semiconductor for pH sensing. *Electrochemistry Communications* **2020,** *116*, 106763.

60. Alihosseini, F.; Sun, G., 17 - Antibacterial colorants for textiles. In *Functional Textiles for Improved Performance, Protection and Health*, Pan, N.; Sun, G., Eds. Woodhead Publishing: 2011; pp 376-403.
61. López, J. In *The transition from natural madder to synthetic alizarine in the American textile industry, 1870-1890*, 1989.
62. Lee, J.-M.; Kim, M.-G.; Byun, J.-H.; Kim, G.-C.; Ro, J.-H.; Hwang, D.-S.; Choi, B.-B.; Park, G.-C.; Kim, U.-K., The effect of biomechanical stimulation on osteoblast differentiation of human jaw periosteum-derived stem cells. *Maxillofacial Plastic and Reconstructive Surgery* **2017,** *39* (1), 7.
63. Kannan, S.; Ghosh, J.; Dhara, S. K., Osteogenic differentiation potential of porcine bone marrow mesenchymal stem cell subpopulations selected in different basal media. *Biology Open* **2020,** *9* (10).
64. Kubo, Y.; Ishida, T.; Kobayashi, A.; James, T. D., Fluorescent alizarin–phenylboronic acid ensembles: design of self-organized molecular sensors for metal ions and anions. *Journal of Materials Chemistry* **2005,** *15* (27-28), 2889-2895.
65. Aghaei, Z.; Emadzadeh, B.; Ghorani, B.; Kadkhodaee, R., Cellulose Acetate Nanofibres Containing Alizarin as a Halochromic Sensor for the Qualitative Assessment of Rainbow Trout Fish Spoilage. *Food and Bioprocess Technology* **2018,** *11* (5), 1087-1095.
66. Zaggout, F. R.; Qarraman, A. E.-F. A.; Zourab, S. M., Behavior of immobilized Alizarin Red S into sol–gel matrix as pH sensor. *Materials Letters* **2007,** *61* (19), 4192-4195.
67. Shalaby, A. A.; Mohamed, A. A., Determination of acid dissociation constants of Alizarin Red S, Methyl Orange, Bromothymol Blue and Bromophenol Blue using a digital camera. *RSC Advances* **2020,** *10* (19), 11311-11316.
68. Swamy, B. E. K.; Chandra, U.; Bodke, Y. D.; Vasanth, K. L.; Pai, K. V. In *Cyclic Voltammetric Investigations of Alizarin at Carbon Paste Electrode using Surfactants*, 2009.
69. Singh, M.; Patkar, R. S.; Vinchurkar, M.; Baghini, M. S., Cost Effective Soil pH Sensor Using Carbon-Based Screen-Printed Electrodes. *IEEE Sensors Journal* **2020,** *20* (1), 47-54.
70. Dai, C.; Song, P.; Wadhawan, J. D.; Fisher, A. C.; Lawrence, N. S., Screen Printed Alizarin-Based Carbon Electrodes: Monitoring pH in Unbuffered Media. *Electroanalysis* **2015,** *27* (4), 917-923.
71. Zamora, M. L.; Dominguez, J. M.; Trujillo, R. M.; Goy, C. B.; Sánchez, M. A.; Madrid, R. E., Potentiometric textile-based pH sensor. *Sensors and Actuators B: Chemical* **2018,** *260*, 601-608.
72. Fernández-Caramés, T. M.; Fraga-Lamas, P., Towards The Internet of Smart Clothing: A Review on IoT Wearables and Garments for Creating Intelligent Connected E-Textiles. *Electronics* **2018,** *7* (12), 405.
73. Islam, G. M. N.; Ali, A.; Collie, S., Textile sensors for wearable applications: a comprehensive review. *Cellulose* **2020,** *27* (11), 6103-6131.
74. Tseghai, G. B.; Mengistie, D. A.; Malengier, B.; Fante, K. A.; Van Langenhove, L., PEDOT:PSS-Based Conductive Textiles and Their Applications. *Sensors* **2020,** *20* (7), 1881.
75. Sánchez-Jiménez, M.; Estrany, F.; Borràs, N.; Maiti, B.; Díaz Díaz, D.; del Valle, L. J.; Alemán, C., Antimicrobial activity of poly(3,4-ethylenedioxythiophene) n-doped with a pyridinium-containing polyelectrolyte. *Soft Matter* **2019,** *15* (38), 7695-7703.
76. Talikowska, M.; Fu, X.; Lisak, G., Application of conducting polymers to wound care and skin tissue engineering: A review. *Biosensors and Bioelectronics* **2019,** *135*, 50-63.
77. Nassar, J. M.; Cordero, M. D.; Kutbee, A. T.; Karimi, M. A.; Sevilla, G. A. T.; Hussain, A. M.; Shamim, A.; Hussain, M. M., Paper Skin Multisensory Platform for Simultaneous Environmental Monitoring. *Advanced Materials Technologies* **2016,** *1* (1), 1600004-n/a.
78. Gou, P.; Kraut, N. D.; Feigel, I. M.; Bai, H.; Morgan, G. J.; Chen, Y.; Tang, Y.; Bocan, K.; Stachel, J.; Berger, L.; Mickle, M.; Sejdić, E.; Star, A., Carbon Nanotube Chemiresistor for Wireless pH Sensing. *Scientific Reports* **2014,** *4* (1), 4468.

79. Pang, F.-F.; Li, S.; Sun, W.-Q.; Han, G.-Z., Reversible conductivity modulation of PEDOT:PSS based on pH. *Materials Chemistry and Physics* **2017,** *186*, 246-250.
80. Mochizuki, Y.; Horii, T.; Okuzaki, H., Effect of pH on Structure and Conductivity of PEDOT/PSS. *Transactions of the Materials Research Society of Japan* **2012,** *37* (2), 307-310.
81. Lin, J.; Peng, Z.; Liu, Y.; Ruiz-Zepeda, F.; Ye, R.; Samuel, E. L. G.; Yacaman, M. J.; Yakobson, B. I.; Tour, J. M., Laser-induced porous graphene films from commercial polymers. *Nature Communications* **2014,** *5* (1), 5714.
82. Pöller, S.; Schuhmann, W., A miniaturized voltammetric pH sensor based on optimized redox polymers. *Electrochimica Acta* **2014,** *140*, 101-107.
83. Makos, M. A.; Omiatek, D. M.; Ewing, A. G.; Heien, M. L., Development and Characterization of a Voltammetric Carbon-Fiber Microelectrode pH Sensor. *Langmuir* **2010,** *26* (12), 10386-10391.
84. Galdino, F. E.; Smith, J. P.; Kwamou, S. I.; Kampouris, D. K.; Iniesta, J.; Smith, G. C.; Bonacin, J. A.; Banks, C. E., Graphite Screen-Printed Electrodes Applied for the Accurate and Reagentless Sensing of pH. *Analytical Chemistry* **2015,** *87* (23), 11666-11672.
85. Lu, M.; Compton, R. G., Voltammetric pH sensing using carbon electrodes: glassy carbon behaves similarly to EPPG. *Analyst* **2014,** *139* (18), 4599-4605.
86. Parrilla, M.; Cuartero, M.; Crespo, G. A., Wearable potentiometric ion sensors. *TrAC Trends in Analytical Chemistry* **2019,** *110*, 303-320.
87. Manjakkal, L.; Dervin, S.; Dahiya, R., Flexible potentiometric pH sensors for wearable systems. *RSC Advances* **2020,** *10* (15), 8594-8617.
88. Song, Y.; Lv, H.; Hu, S.; Yang, C.; Zhu, X., Electroactivity of Polyaniline in High pH Solutions. *Acta Chimica Sinica* **2013,** *71*, 999.
89. Saeb, M. R.; Zarrintaj, P., Chapter 10 - Polyaniline/graphene-based nanocomposites. In *Fundamentals and Emerging Applications of Polyaniline*, Mozafari, M.; Chauhan, N. P. S., Eds. Elsevier: 2019; pp 165-175.
90. Wang, L.; Lu, X.; Lei, S.; Song, Y., Graphene-based polyaniline nanocomposites: preparation, properties and applications. *Journal of Materials Chemistry A* **2014,** *2* (13), 4491-4509.
91. Yoon, H.; Nah, J.; Kim, H.; Ko, S.; Sharifuzzaman, M.; Barman, S. C.; Xuan, X.; Kim, J.; Park, J. Y., A chemically modified laser-induced porous graphene based flexible and ultrasensitive electrochemical biosensor for sweat glucose detection. *Sensors and Actuators B: Chemical* **2020,** *311*, 127866.
92. Huang, L.; Su, J.; Song, Y.; Ye, R., Laser-Induced Graphene: En Route to Smart Sensing. *Nano-Micro Letters* **2020,** *12* (1), 157.
93. Liu, S.; Zhang, X.; Zhang, L.; Xie, W., Ultrasonic spray coating polymer and small molecular organic film for organic light-emitting devices. *Scientific Reports* **2016,** *6* (1), 37042.
94. Stryckers, J.; D'Olieslaeger, L.; Silvano, J. V. M.; Apolinario, C. K.; Laranjeiro, A. C. G.; Gruber, J.; D'Haen, J.; Manca, J.; Ethirajan, A.; Deferme, W., Layer formation and morphology of ultrasonic spray coated polystyrene nanoparticle layers. *physica status solidi (a)* **2016,** *213* (6), 1441-1446.
95. Torah, R.; Wei, Y.; Li, Y.; Yang, K.; Beeby, S.; Tudor, J., Printed Textile-Based Electronic Devices. In *Handbook of Smart Textiles*, Tao, X., Ed. Springer Singapore: Singapore, 2015; pp 653-687.
96. Kipphan, H., *Handbook of Print Media: Technologies and Production Methods*. Springer-Verlag New York, Inc.: 2006.
97. Farooqui, M. F.; Shamim, A., Low Cost Inkjet Printed Smart Bandage for Wireless Monitoring of Chronic Wounds. *Scientific Reports* **2016,** *6*, 28949.
98. Jiang, H.-Y.; Hu, X.-D.; Zhu, J.-J.; Wan, J.; Yao, J.-B., Studies on the photofading of alizarin, the main component of madder. *Dyes and Pigments* **2021,** *185*, 108940.
99. Ye, R.; James, D. K.; Tour, J. M., Laser-Induced Graphene: From Discovery to Translation. *Advanced Materials* **2019,** *31* (1), 1803621.

100. Ferrari, A. C.; Meyer, J. C.; Scardaci, V.; Casiraghi, C.; Lazzeri, M.; Mauri, F.; Piscanec, S.; Jiang, D.; Novoselov, K. S.; Roth, S.; Geim, A. K., Raman Spectrum of Graphene and Graphene Layers. *Physical Review Letters* **2006,** *97* (18), 187401.
101. Manjakkal, L.; Shakthivel, D.; Dahiya, R., Flexible Printed Reference Electrodes for Electrochemical Applications. *Advanced Materials Technologies* **2018,** *3* (12), 1800252.
102. Wan, M., Absorption spectra of thin film of polyaniline. *Journal of Polymer Science Part A: Polymer Chemistry* **1992,** *30* (4), 543-549.
103. Tehrani, Z.; Whelan, S. P.; Mostert, A. B.; Paulin, J. V.; Ali, M. M.; Ahmadi, E. D.; Graeff, C. F. O.; Guy, O. J.; Gethin, D. T., Printable and flexible graphene pH sensors utilising thin film melanin for physiological applications. *2D Materials* **2020,** *7* (2), 024008.
104. Bocchini, S.; Castellino, M.; Della Pina, C.; Rajan, K.; Falletta, E.; Chiolerio, A., Inkjet printed doped polyaniline: Navigating through physics and chemistry for the next generation devices. *Applied Surface Science* **2018,** *456*, 246-258.
105. Rahimi, R.; Brener, U.; Chittiboyina, S.; Soleimani, T.; Detwiler, D. A.; Lelièvre, S. A.; Ziaie, B., Laser-enabled fabrication of flexible and transparent pH sensor with near-field communication for in-situ monitoring of wound infection. *Sensors and Actuators B: Chemical* **2018,** *267*, 198-207.
106. Sinha, S. K.; Noh, Y.; Reljin, N.; Treich, G. M.; Hajeb-Mohammadalipour, S.; Guo, Y.; Chon, K. H.; Sotzing, G. A., Screen-Printed PEDOT:PSS Electrodes on Commercial Finished Textiles for Electrocardiography. *ACS applied materials & interfaces* **2017,** *9* (43), 37524-37528.
107. Sico, G.; Montanino, M.; De Girolamo Del Mauro, A.; Imparato, A.; Nobile, G.; Minarini, C., Effects of the ink concentration on multi-layer gravure-printed PEDOT:PSS. *Organic Electronics* **2016,** *28*, 257-262.
108. Basak, I.; Nowicki, G.; Ruttens, B.; Desta, D.; Prooth, J.; Jose, M.; Nagels, S.; Boyen, H.-G.; D'Haen, J.; Buntinx, M.; Deferme, W., Inkjet Printing of PEDOT:PSS Based Conductive Patterns for 3D Forming Applications. *Polymers* **2020,** *12* (12).
109. Morgan, M. L.; Curtis, D. J.; Deganello, D., Control of morphological and electrical properties of flexographic printed electronics through tailored ink rheology. *Organic Electronics* **2019,** *73*, 212-218.
110. Miriani, R. M.; Abidian, M. R.; Kipke, D. R. In *Cytotoxic analysis of the conducting polymer PEDOT using myocytes*, 2008 30th Annual International Conference of the IEEE Engineering in Medicine and Biology Society, 20-25 Aug. 2008; 2008; pp 1841-1844.
111. Park, H. J.; Yoon, J. H.; Lee, K. G.; Choi, B. G., Potentiometric performance of flexible pH sensor based on polyaniline nanofiber arrays. *Nano Convergence* **2019,** *6* (1), 9.
112. Guinovart, T.; Valdés-Ramírez, G.; Windmiller, J. R.; Andrade, F. J.; Wang, J., Bandage-Based Wearable Potentiometric Sensor for Monitoring Wound pH. *Electroanalysis* **2014,** *26* (6), 1345-1353.
113. Wang, R.; Zhai, Q.; Zhao, Y.; An, T.; Gong, S.; Guo, Z.; Shi, Q.; Yong, Z.; Cheng, W., Stretchable gold fiber-based wearable electrochemical sensor toward pH monitoring. *Journal of Materials Chemistry B* **2020,** *8* (16), 3655-3660.
114. Stempien, Z.; Rybicki, T.; Rybicki, E.; Kozanecki, M.; Szynkowska, M. I., In-situ deposition of polyaniline and polypyrrole electroconductive layers on textile surfaces by the reactive ink-jet printing technique. *Synthetic Metals* **2015,** *202*, 49-62.
115. Edberg, J.; Brooke, R.; Hosseinaei, O.; Fall, A.; Wijeratne, K.; Sandberg, M., Laser-induced graphitization of a forest-based ink for use in flexible and printed electronics. *npj Flexible Electronics* **2020,** *4* (1), 17.
116. Kwon, S.; Lee, T.; Choi, H.-J.; Ahn, J.; Lim, H.; Kim, G.; Choi, K.-B.; Lee, J., Scalable fabrication of inkless, transfer-printed graphene-based textile microsupercapacitors with high rate capabilities. *Journal of Power Sources* **2021,** *481*, 228939.

TOC File

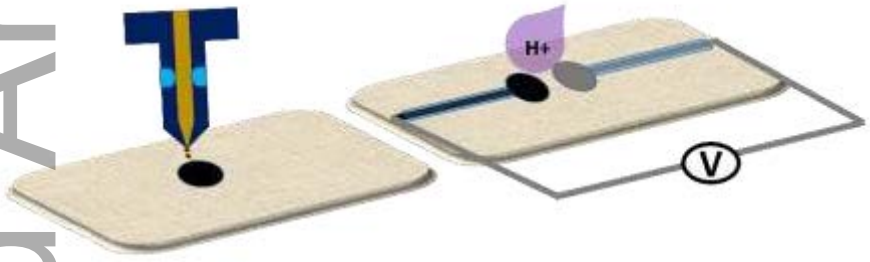

This article demonstrates the development of pH sensing devices on textiles conceptually and experimentally for a physiologically relevant range of pH measurements. The work primarily focussed on the multiple aspects of fabrication, materials, substrates, sensing performance and measurement technology. The literature background and experimental investigation helped to identify the most suitable fabrication strategy leading to the development of mass producible printed pH sensors on textiles with excellent repeatability and sensitivity.